Chapter 2
Functional Properties of Organic Cation Transporter OCT1, Binding of Substrates and Inhibitors, and Presumed Transport Mechanism

Hermann Koepsell and Thorsten Keller

Abstract Organic cation transporters (OCTs) of the SLC22 family mediate absorption, distribution and excretion of cationic drugs. The OCTs belong to the major facilitator superfamily (MFS) containing transporters with 12 pseudosymmetrically arranged transmembrane α-helices. Whereas most transporters of the MFS are substrate selective and secondary active, most transporters of the SLC22 family are polyspecific facilitative diffusion systems. Recently resolved crystal structures of MFS transporters indicate translocation via alternating access surpassing a state with substrate occlusion. After cloning of the rat transporters rOCT1 and rOCT2, the functional properties of these transporters have been investigated employing tracer uptake measurements, electrical measurements, voltage clamp fluorometry, and substrate binding measurements. Extensive mutagenesis studies in rOCT1 were interpreted in frame of tertiary structures that were modeled according to lactose permease which belongs to the MFS. Considering rOCT1 and rOCT2 as OCT prototypes, and assuming that all transporters of the MFS undergo similar interhelical movements during transport, a model for the translocation mechanism of OCTs is proposed. The model suggests that two small organic cations bind to the innermost cleft of the outward-facing conformation of OCTs and that translocation can be performed when either one or two cations are loaded per transporter monomer. With this model recent experimental recent results concerning interaction of ligands at OCTs can be explained that have high biomedical impact for in vitro testing.

Keywords Organic cation transporters • OCT1 • SLC22 • MFS • Transport mechanism • Polyspecificity • Mutagenesis • Tertiary structure • Modeling

H. Koepsell (✉) • T. Keller
Department of Molecular Plant Physiology and Biophysics, Julius-von-Sachs-Institute, University of Würzburg, Julius-von-Sachs Platz 2, 97082 Würzburg, Germany
e-mail: Hermann@koepsell.de

© Springer International Publishing Switzerland 2016

G. Ciarimboli et al. (eds.), *Organic Cation Transporters*,
DOI 10.1007/978-3-319-23793-0_2

Introduction

The organic cation transporters OCT1, OCT2 and OCT3 of the *SLC22* transporter family are polyspecific facilitative diffusion systems with overlapping substrate specificities [1–3]. The *SLC22* family belongs to the major facilitator superfamily (MFS) which represents the second largest superfamily of transporters following the superfamily of ABC transporters [4]. The MFS contains secondary active cotransporters and antiporters and facilitative diffusion systems including the OCTs. The driving force for transport by OCTs is provided by the concentration difference of the respective cationic substrate across the plasma membrane and the electrical membrane potential. Because OCTs can mediate uniport of organic cations across the plasma membrane, their translocation of cations can be analysed by electrical measurements.

The purpose of the present article is to discuss the current knowledge concerning substrate recognition and transport mechanism of OCTs and to provide a comprehensible hypothesis for substrate recognition and transport mechanism of OCTs that includes very recent findings. In a first part we summarize the characterization of transport by rat organic cation transporters rOCT1 and rOCT2 and present experimental evidence which indicates that translocation by OCTs occurs by an alternating access transport mechanism. Because the current molecular understanding of functions of OCTs is mainly based on extensive mutagenesis of rOCT1 and on crystal structures of transporters of the MFS in different conformations, we included a second part in which we discuss the interpretation of mutagenesis experiments in general and the benefits and limitations of structural models of OCTs that are performed on the basis of crystal structures of MFS transporters. In this part we also present the current concept of alternating access transport mechanism by transporters of the MFS. In a third part of the review, current knowledge about structure-function relationship of rOCT1 is presented which is derived from functional characterizations of rOCT1 mutants in combination with models of tertiary structures in the outward-facing and inward-facing conformation. In this part we describe mapping of cation binding sites, elucidation of quaternary structure and transporting unit, measurements of transport-related structural changes, identification of a structural key element for translocation, and identification of high affinity binding sites. We also mention some of our very recent data concerning the identification of MPP binding sites in the innermost part of the outward-facing binding cleft that have not been published so far. In the fourth part of the review we provide a model for substrate binding and translocation that is derived from the described functional data. In this part we point out how recent experiments indicating that inhibitor affinities are dependent on substrate concentration and substrate structure, can be explained within the new model.

Functional Properties of rOCT1 and rOCT2

Substrate and Inhibitor Selectivity

OCT1, OCT2 and OCT3 have been cloned from different species including human and have been characterized functionally [1–3]. Different selectivities of substrates and inhibitors were observed between OCT1, OCT2 and/or OCT3 within individual species and for the individual OCT subtypes between different species. The functional characterizations are consistent with the view that independent of species the three OCT subtypes have the same basic properties. This includes the independence from sodium gradient, transport in both directions, and the possibility to function as electrogenic uniporter or electroneutral exchanger. This may be an over-simplified view because an in depth characterization of transporter properties has only been performed for rOCT1 and rOCT2, and data were obtained suggesting that the stoichiometry between translocation of charges and organic cations is different between rOCT1 and rOCT2 [5]. Similar to all OCTs characterized so far, rOCT1 and rOCT2 translocate organic cations with widely differing molecular structures and are inhibited by a large number of compounds that are not transported [6]. Tetraethylammonium (TEA), 1-methyl-4-phenyl-pyridinium (MPP), ^{1}*N*-methylnicotinamide, histamine, choline and *d*-tubericidine are transported by rOCT1 and rOCT2 with similar apparent K_m values [7, 8]. At variance guanidine and dopamine are common substrates of rOCT1 and rOCT2, however, 10-fold and 40-fold lower apparent K_m values have been determined for rOCT1 versus rOCT2, respectively [7, 9]. Quinine and serotonin are transported by rOCT1 but not by rOCT2 [6]. Whereas tetrapropylammonium (TPrA), tetrapentylammonium (TPeA) and desipramine are common inhibitors of rOCT1 and rOCT2 with similar IC_{50} values, corticosterone inhibits rOCT2 with a 38-fold lower IC_{50} value compared to rOCT1, and procainamide inhibits rOCT2 with a 68-fold higher IC_{50} [7]. Evidence has been presented that both rOCT1 and rOCT2 translocate organic cations in an electrogenic manner when they operate under *trans*-zero conditions as uniporters, whereas cation transport is electroneutral when they operate in the cation exchange mode [7, 10–13]. It has been shown that both rOCT1 and rOCT2 operate independently from sodium and chloride, and data were obtained suggesting that they function independently of proton gradients [10, 12–14].

Stoichiometry Between Translocation of Charge and Cations

The stoichiometry of rOCT1 between translocated cations and charges appears to be different compared to rOCT2. For tracer uptake of TEA, choline and MPP by rOCT1 and rOCT2 similar V_{max} values were obtained, however, the currents induced

by saturating concentrations of these compounds were up to ten times smaller in oocytes expressing rOCT1 versus rOCT2. This difference is supposed to be due to a translocation of small cations together with organic cation substrates by rOCT2. Measuring rOCT2 mediated translocation of organic cations in parallel with translocation of positive charge, translocation of a surplus of positive charge was observed at low membrane potential [5]. This surplus of charge translocation could not be explained by leakage for small ions during the transport cycle. It was dependent on the presence of a negatively charged amino acid within the innermost part of the modeled outward-open binding pocket of rOCT2 which is not conserved in rOCT1 [5].

Demonstration of Transporter Function

The findings that one subtype of the SLC5 family, SLC5A4 also called SGLT3, is a Na^+-D-glucose cotransporter in pig and a glucose-ligated ion channel in human [15], and that protein EcClC from *Escherichia coli* which has a channel like structure containing a transmembrane path and a selectivity filter functions as Cl^-/H^+ antiporter [16–18], indicate that the structural differences between channels and transporters may be small. However, the functional distinction between channel and transport activity is useful and of theoretical and practical relevance. During transport substrate translocation is stoichiometrically linked to structural changes of the protein which are typically relatively large. Transport always includes binding and dissociation of the substrate which allows a subtle differentiation of substrate selectivity between transporters. In contrast channel activity comprises opening of transmembrane pathways that are controlled by gating mechanisms which include conformational changes in the protein that may be small. The selectivity of channels is determined by selectivity filters. Because open channel pathways may allow passage of a restricted number of ions and may contain binding sites for the translocated ions, channel activity may show saturation similar to transporters. Since rOCT1 and rOCT2 facilitate diffusion of structurally different compounds across the membrane it was important to clarify whether they function as transporters as generally assumed, or as poorly selective channels with short opening times which would explain the relatively low rates of cation translocation.

For rOCT2 mediated TEA^+ induced inward currents in oocytes measured under *trans*-zero condition at −50 mV, a high activation energy of 39 kJ/mol was determined indicating that transporter typical large conformational changes are associated with TEA^+ translocation [14]. Electrical measurements performed with inside-out oriented giant patches from oocytes in which rOCT2 was expressed, strongly support transport function [12]. When 2 mM choline or 10 mM choline were present on both sides of the giant patches and different membrane potentials were applied, symmetrical and potential dependent inward or outward currents were measured (Fig. 2.1a). Importantly, the currents observed with 2 mM choline were higher compared to the currents observed with 10 mM choline. This observation

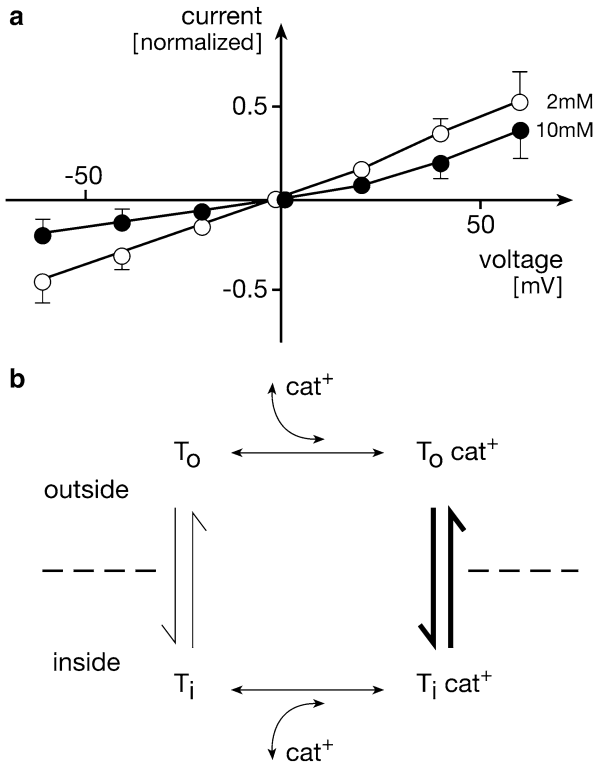

Fig. 2.1 Higher voltage induced currents mediated by rOCT2 with 2 mM choline versus 10 mM choline on both membrane sides indicate electrogenic transport. (**a**) Current–voltage relationship in giant patches from *Xenopus laevis* oocytes in which rOCT2 was expressed and 2 or 10 mM choline were present at both sides of the plasma membrane. (**b**) Simple transporter model allowing electrogenic cation uniport and more rapid electroneutral cation exchange

contradicts channel-like activity because in a channel a higher concentration of choline would lead to higher voltage dependent currents. In contrast the data are consistent with the alternating access transporter model shown in Fig. 2.1b. The model implies two possible transport modes, electrogenic uniport and electroneutral cation exchange. In both modes a cation binds to the outside-facing substrate binding site, the bound cation is exposed to the intracellular side and released. Finally the empty inward-facing substrate binding site is transposed to the extracellular side and a second uniport cycle can be started. In the electroneutral cation exchange mode an intracellular cation binds to the inward-facing substrate binding site and the cation-loaded substrate binding site is exposed to the extracellular site where the counter-transported cation is released. Because the electrogenic transport mode is preferred at low substrate concentration, the higher currents observed with 2 mM choline compared to 10 mM choline are consistent with transport function. Experimental evidence for transport has been also provided by demonstrating *trans-stimulation* of rOCT1 mediated uptake under voltage-clamp condition [13]. These experiments were performed with proteoliposomes containing purified rOCT1 in which the membrane potential was clamped to zero by valinomycin in the presence of equal concentrations of potassium on both sides of the membrane. Under these conditions uptake of radioactive labeled MPP was stimulated when the proteoliposomes were

loaded with choline. This observation is not consistent with channel activity. However, it can be explained by the transport model assuming that the conformational changes of the transporters leading to the in–out orientation of the choline-loaded substrate binding site occurs more rapidly than the structural changes leading to in–out orientation of the empty transporter (Fig. 2.1b).

Experimental support that rOCT2 is a transporter that operates according to the alternating access model [19, 20] was provided by experiments in which rOCT2 mediated transport was inhibited by corticosterone or TBuA that were applied either from the extracellular side of the plasma membrane or from the intracellular side [21]. Competition experiments indicated that both compounds interact within the substrate binding pocket. We characterized the interaction of corticosterone and TBuA with the outward-facing substrate binding pocket of rOCT2 by measuring the short-term inhibition of TEA induced inward-currents in intact oocytes expressing rOCT2, and the interaction with the inward-facing substrate binding pocket by measuring short-term inhibition of TEA induced outward-currents in giant patches obtained from rOCT2 expressing oocytes [21]. Corticosterone had a higher affinity when applied from extracellular compared to intracellular whereas TBuA had a lower affinity from extracellular compared to intracellular. The data indicate that the substrate binding region of rOCT2 can be exposed to both sides of the plasma membrane and exhibits different affinities for substrates and inhibitors in both conformations as postulated for the alternating access transport mode.

Considerations about Interpretation of Functional Effects of Mutations

To unravel functional mechanisms of individual transporters, crystal structures of different functional states and functional characterization of point mutations in critical positions are required. In addition the quaternary structure of the transporter must be known. If the transporter forms dimers or oligomers, it must be known whether the monomers function independently or not. The interpretation of functional effects of point mutations may be straight forward if crystal structures of the same transporter have been solved, whereas the interpretation must remain speculative if no crystal structure is available. In this situation modeling of tertiary structures according to known structures from transporters of the same family or superfamily are helpful for interpretation.

Changes of V_{max} values measured after overexpression of mutants in cells are difficult to interprete if the exchanged amino acid is not located in a functionally relevant domain of the crystallized or modeled transporter. Reasons are that the exchange of amino acids within parts of transporters that are not directly involved in substrate recognition and/or transport but are important for the formation of the correct tertiary structure, may result in ineffective targeting to the plasma membrane and/or to an inactive or partially active misfolded transporter within the membrane. An additional difficulty is that the available methods to determine the amount of

transporter incorporated into the plasma membrane do not allow the identification of small differences. Measurements of V_{max} values after reconstitution of transporters in proteoliposomes circumvent the problem of the potential effect of mutations on targeting.

Similar to V_{max}, changes of apparent K_m values observed after point mutations are difficult to interprete when the crystal structure has not been solved. One reason is that the apparent K_m is a bulk constant that may be influenced by rate constants of different steps during translocation including substrate binding at the extracellular side and substrate release at the intracellular side. In case of a cotransporter in which the binding of the cosubstrate increases the affinity for substrate binding, effects of mutations on the binding of the cosubstrate or on the allosteric effect of cosubstrate binding may change the apparent K_m. In addition to these obstacles for correct interpretation it must be kept in mind that point mutations in peripheral parts of a transporter may induce structural changes that lead to alterations of the apparent K_m. In case of polyspecific transporters effects of point mutations on K_m values of different substrates can be determined in order to evaluate effects on selectivity, however, also in this case a solid interpretation is only possible in combination with a crystal structure and a modeled structure is required to raise educated hypotheses.

If point mutations alter IC_{50} values determined for non-transported competitive inhibitors measured in cells, it can be concluded that the structure of the substrate binding site has been altered directly or indirectly. In case of polyspecific transporters differential effects of point mutations on IC_{50} values for different substrates are of specific interest. Such type of investigations may provide indirect support for the interaction of substrates and inhibitors with different binding sites in a binding region that may be overlapping (see below). In such a scenario it has to be kept in mind that allosteric interactions between binding of substrates and inhibitors may occur. Again a modeled tertiary structure of the binding cleft may help to raise hypotheses.

The analysis of partial reactions of the transport cycles after point mutations has high impact for the elucidation of transport mechanisms. These studies include direct measurements of binding of substrates, cosubstrates and inhibitors, determinations of stoichiometries between substrate and cosubstrate or translocation of charged substrate and charge, effects of substrate induced conformational changes etc. In combination with crystal structures these types of studies are required to unravel transport mechanism. In combination with modeled structures such types of studies are helpful for generation of hypotheses.

Considerations about Modeling of OCT Structures According to Crystal Structures of MFS Transporters

So far 16 crystal structures of transporters from MFS have been reported. Although the different transporters have less than 20 % amino acid identity between each other, they all exhibit the same pseudosymmetric structure consisting of an

N-terminal and a C-terminal part, each comprising six TMHs. Five different structural states of MFS transporters have been crystallized; an open outward-facing state (fucose transporter FucP from *E. coli* [22]), a ligand-bound, outward-facing, partially occluded state (xylose transporter XylE from *E. coli* [23]), an occluded state (oxalate transporter OxlT from *Oxalobacter formigenes* [24], multidrug transporter EmrD from *E. coli* [25], nitrate/nitrite transporter NarU from *E. coli* [26]), an inward-facing occluded state (phosphate transporter PiPT from *Piriformospora indica* [27], peptide transporter PepTso from *Shevanella oneidensis* [28]), and an open inward-facing state (the lactose permease from LacY *E. coli* [29–32], glycerol-3-phosphate transporter GlpT from *E. coli* [33], peptide transporter $PepT_{St}$ from *Streptococcus thermophilis* [34], peptide transporter $PepT_{So2}$ from *S. oneidensis* [35], peptide transporter GkPOT from *Geobacillus kaustophilus* [36], nitrate/nitrite transporter NarK from *E. coli* [37], and nitrate transporter NRT1.1 from *Arabidopsis* [38]). Whereas the open outward-facing and the open inward-facing state are mainly formed by en-block movements of the pseudosymmetric transporter halfs without significant bending of individual TMHs, the formation of the occluded states required bending and movements of individual helices in addition to en bloc movements of transporter halfs. The large overall similarities between the crystal structures of different transporters including proton-cotransporters, a sodium-cotransporter and polyspecific facilitative diffusion systems suggest that the MFS transporters have a common basic structure that allows the alternating access related conformational transitions that have been described as rocker-switch movement of the two transporter halfs [39]. The functional difference between the transporters are supposed to be due to transporter specific structural differences in the binding sites, in regions that are responsible for energy coupling and in regions that form the translocation pathways. In conclusion a modeling of the tertiary structure of OCTs on the basis of MFS transporters is expected to provide the structural backbone of OCTs allowing alternating access but cannot provide details explaining polyspecifc translocation of cations by facilitative diffusion.

Theoretical Considerations About Polyspecificity of OCTs

Accepting that OCTs are transporters that operate in the alternating access mode, polyspecificity must be explained by polyspecific cation binding that induces transporter related conformational changes rather than by poorly discriminative selectivity filters. Although allosteric changes within the substrate binding regions of polyspecifc transporters are expected after binding of a specific substrate, it can be excluded that the potential of rOCT1 and rOCT2 to bind structurally different cations like TEA and MPP is mainly due to an induced fit mechanism. In the absence of pre-existing binding sites for TEA and MPP, the interaction energy between the cations and the binding region is supposed to be too low to induce a structural change within the binding pocket that could form a selective binding site exhibiting tight interaction with the respective cation. In addition the tertiary structure of the

transporters is supposed to restrict the degrees of freedom allowing substrate induced structural changes that would be required to induce polyspecificity. In conclusion, polyspecific binding to OCTs is supposed to require cation binding to several binding sites that interact with different ligand structures. These binding sites may be located within a binding region as has been demonstrated for p-glycoprotein [40, 41]. An intriguing question is how binding at different sites can induce the conformational changes that mediate cation translocation or in other words how ligand protein interaction at different sites can provide the activation energy to overcome the activation barrier for translocation [42, 43].

Initial Mutagenesis Experiments in rOCT1

We started our mutagenesis analysis of rOCT1 by exchanging amino acids of rOCT1 which are conserved in OCTs but not found in the organic anion transporters (OATs) of the *SLC22* family [44]. In another study we replaced all amino acids of the fourth TMH that contains many amino acids that are conserved in the OCTs [45]. For functional characterization we expressed the rOCT1 mutants in oocytes of *Xenopus laevis* and compared K_m and V_{max} values for different substrates as well as IC_{50} values for inhibition of TEA and/or MPP uptake by transported as well as non-transported inhibitors. To identify effects of mutations on transporter targeting to the plasma membrane we performed Western blots of isolated plasma membranes. The experiments revealed that the replacement of aspartate 475 in the 11th TMH of rOCT1 by glutamate reduced the amount of transporter in the plasma membrane by 90 % and decreased the apparent K_m value for TEA eightfold whereas the apparent K_m value for MPP was not changed. Similar to the K_m for TEA the IC_{50} values for the competitive non transported inhibitors TBuA, tetrapropylammonium (TPrA) and tetrapentylammonium (TPeA) were decreased. We interpreted that aspartate 475 is probably directly involved in binding of TEA, TBuA, TPrA and TPeA. Because rOCT1 mediated transport of TEA is competitively inhibited by MPP and vice versa, we interpreted that rOCT1 probably contains a substrate binding region with overlapping binding domains for TEA and MPP. Conservative replacements of 18 amino acids in the fourth TMH revealed that after replacement of Trp218 by tyrosine (W218Y) and Tyr222 by leucine (Y222L) the K_m values of both TEA and MPP were decreased whereas after replacement of Tyr222 by phenylalanine (Y222F) only the K_m value for TEA and after replacement of Thr226 by alanine (T226A) only the K_m value for MPP was decreased. Presuming that the K_m values were reflecting the affinity of substrate binding to the outward-facing conformation of rOCT1, these data supported the existence of an outward-facing binding region with overlapping binding domains for TEA and MPP. The data did not allow to differentiate whether Trp218, Tyr222 or Thr226 are directly involved in binding of TEA and/or MPP or whether the mutations in these positions altered the structure of the substrate binding domains.

Employing the nearly 40-fold higher affinity of corticosterone for inhibition of cation uptake by rOCT2 versus rOCT1, we identified the amino acids which are responsible for this difference. When amino acids Ala443, Leu447 and Gln448 of rOCT1 were replaced by the respective amino acids of rOCT2 (Ile443, Tyr447, Glu448), corticosterone inhibited cation uptake of the rOCT1 mutant with the same affinity as rOCT2 wildtype [46]. The measurements were performed by expressing the transporters in *X. oocytes* and measuring the effects of corticosterone on the uptake of 10 μM TEA or 0.1 μM MPP using an incubation time of 30 min. Although corticosterone is not transported by rOCT1 or rOCT2 we could not differentiate whether the observed inhibition occured from extracellular or intracellular, because corticosterone passively permeates the plasma membrane. Considering also that the amino acid exchanges may exhibit indirect effects on the extracellular and/or intracellular corticosterone binding site(s), the data did not provide unequivocal information about the binding site(s) for corticosterone. Because the triple rOCT1 mutant (A443I,L447Y,Q448E) showed decreased apparent K_m values for TEA and MPP, and the IC_{50} values for corticosterone inhibition of TEA uptake versus MPP uptake were different, the data suggested complex interactions between substrate and corticosterone binding sites.

Modeling and Mapping of the Open, Inward-Facing Binding Cleft of rOCT1

2003 the first two high-resolution crystal structures of transporters of the MFS family were published; the glycerol-3-phosphate transporter GlpT from *E. coli* [33] and lactose permease LacY from *E. coli* [29]. Both transporters were crystallized in the open, inward-facing conformation. Using the crystal structure of LacY as template, we modeled rOCT1 in this conformation. The modeled open, inward-facing cleft was formed by TMHs 1, 2, 4 and 5 of the left transporter half and TMHs 7, 8, 10 and 11 of the pseudosymmetric right transporter half (Fig. 2.2c). TMHs 1, 4, 7 and 8 contained distinct bends whereas the other cleft forming TMHs were straight or showed minor bending. In the model Asp475 in TMH 11, Phe160 in TMH 2, Tryp218 in TMH 4, and Arg440 in TMH 10 are localized relatively close together in the innermost part of the inward-facing cleft whereas Tyr222 in TMH 4 and Gln448 in TMH 10 are located more peripheral close to the cytosol (Fig. 2.2c). According to the modeled cleft all identified amino acids with the exception of Gln448 have contact with the aqueous phase. Viewing from intracellular into the inward-facing cleft suggests different compartments within the cleft (Fig. 2.2d).

For characterization of the inward-facing cleft by mutagenesis, we measured whether the inhibition of TEA induced inward-currents by intracellular corticosterone was changed after replacement of Leu447 by tyrosine or of Gln448 by glutamate which had been shown to influence the affinity of corticosterone [46, 47]. The mutations in both positions decreased the IC_{50} values for corticosterone suggesting

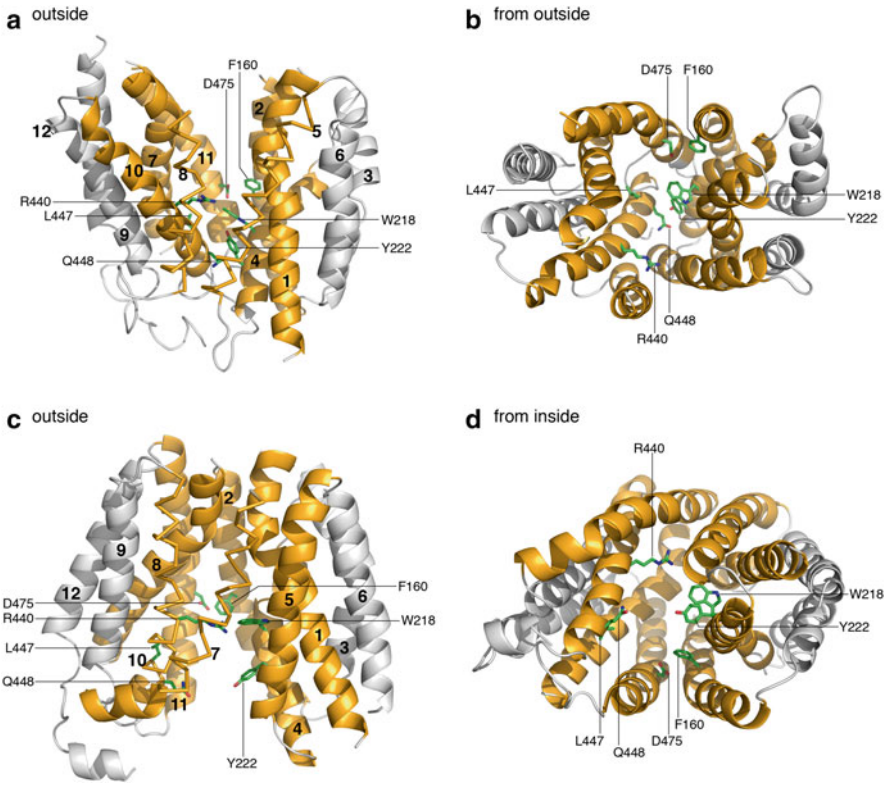

Fig. 2.2 Modeled rOCT1 conformations with outward-facing or inward-facing substrate binding clefts. (**a**) Outward-facing conformation, side view, (**b**) Outward-facing conformation, view from extracellular, (**c**) Inward-facing conformation (side view), (**d**) Inward-facing conformation, view from intracellular. The TMHs forming the cleft are indicated in *orange*. Amino acids that have been identified to be critical substrate affinity, affinity of inhibitors and/or transport are indicated. The TMHs are *numbered*

that corticosterone interacts with the substrate binding domain. These mutations were performed in mutant rOCT1(C451M) which showed higher cation induced currents compared to rOCT1 wildtype [48]. To measure inhibition of TEA induced inward currents by intracellular corticosterone, oocytes were clamped to −50 mV, equilibrated for 10 min with corticosterone, washed for 1 min, and TEA-induced inward currents were measured by superfusion for 45 s with TEA. Trying to further define the interaction site for corticosterone we performed docking experiments of corticosterone with the modeled inward-facing cleft [47]. The obtained data suggest interaction of corticosterone with Phe160 (TMH 2), Trp218 (TMH 4), Arg440 (TMH 10) Leu447 (TMH 10), and Asp475 (TMH 11). Mutagenesis of Phe160, Trp218, Arg440 or Asp475 revealed that the affinity for inhibition of TEA uptake by intracellular corticosterone was increased after replacement of Phe160 by alanine and after replacement of Asp475 by glutamate, whereas maximal inhibition of

TEA uptake by intracellular corticosterone was decreased after replacement of Trp218 by phenylalanine and Arg440 by lysine. Taking together the data indicate that the mutations of Phe160, Trp218, Arg440, Leu447 and Asp475 change the interaction of corticosterone from intracellular either directly or by short-distance allosteric effects. They support the modeled inward-facing cleft. Relevance of Phe160, Trp218, Arg440 and Leu447 for cation translocation was shown by demonstrating that the affinity of MPP to inhibit TEA uptake was changed by mutations in these positions. Noteworthy Phe160 and Arg440 are located within the inner most part of the cleft in about the same plane as Trp218 and Asp475 (Fig. 2.2c).

Modeling and Mapping of the Open, Outward-Facing Binding Cleft of rOCT1

The open, outward-facing cleft of rOCT1 was modeled by applying the en-bloc rearrangement mechanism of the two pseudosymmetric halfs of the modeled inward-facing conformation of rOCT1 as has been proposed for conformational change of LacY during transport [49, 50] (Fig. 2.2a, b). In the outward-facing cleft Phe160, Arg440 and Asp475 are located within the inner third of the outward-facing cleft about in the center of the presumed plasma membrane. Noteworthy, Gln448 and Tyr222 are located at the bottom of the cleft about 20 Å closer to the cytosolic surface of the plasma membrane (Fig. 2.2a) suggesting that cation occlusion may occur in the space between these two different groups of amino acids. Trp218 is located within this space. The top view from extracellular into the cleft (Fig. 2.2b) suggests a division into three compartments lined by Asp475, Trp218 and Phe160, by Asp475, Trp218 and Leu447, or by Tyr222, Glu448 and Arg440.

For characterization of the outward-facing cleft we measured the effects of mutations of Phe160, Trp218, Arg440, Leu447 or Asp475 on the inhibition of TEA or MPP uptake by extracellular corticosterone [47]. The K_i values for inhibition were changed after replacement of Phe160 by alanine, Leu447 by tyrosine and Asp475 by glutamate, whereas the maximal inhibition was reduced after replacement of Trp218 by phenylalanine and Arg440 by lysine. The data indicate that the mutations alter the interaction of corticosterone within the outward-facing binding cleft. The data support the modeled outward-facing cleft.

Elucidation of Quaternary Structure and Transporting Unit of rOCT1

To interprete the effects of the point mutations in rOCT1 on affinities and maximal inhibition of cation uptake correctly, the quaternary structure of rOCT1 and the functional unit for cation transport must be known. MFS transporters may exist as

monomers in the plasma membrane or may form dimers or oligomers which may function independently or in concert. LacY and the sugar/phosphate antiporter UhpT from *E. coli* are present as monomers [51, 52] whereas the reduced folate carrier RFC from human is present as homooligomer in which the monomers function independently [53]. Lactose transport protein LacS from *Streptococcus thermophilus* forms dimers which are required for proton driven lactose uptake [54]. Homo-oligomerization was demonstrated for human organic anion transporter hOAT1 [55] for rat OAT1, rOCT1, rOCT2 [56, 57] and human OCT2 (hOCT2) [58]. It has been also reported that surface expression of hOAT1 and hOCT2 was reduced when oligomerization was disturbed [58, 59]. In addition it was shown that the tertiary structure of the large extracellular loop between TMH 1 and 2 of rOCT1 or hOCT2, which is stabilized by disulfide bridges, is essential for oligomerization [57, 58]. We provided evidence that both monomers of rOCT1 may transport independently under *trans*-zero conditions by showing that the apparent K_m values for TEA and MPP uptake remained unchanged when oligomerization was prevented, and that a tandem protein containing two rOCT1 monomers showed about 50 % transport activity with unchanged K_m values when one monomer was blocked [57]. Cooperativity of monomers concerning transport of other substrates, cation exchange or inhibition of transport has not been excluded.

Analysis of Transport-Related Structural Changes of rOCT1

Employing capacitance measurements with oocytes expressing rOCT2 or an rOCT1 variant with increased electrical activity, substrate and inhibitor dependent movement of charges within the proteins were detected [14, 50]. Since the capacitance changes were also observed with the uncharged inhibitor corticosterone, they are due to charge movements of charged amino acids of the transporter proteins indicating structural changes. Similar capacitance changes were observed with the non-transported inhibitor TBuA and transported cations. This suggests that the observed structural changes in response to transported cations are induced by the initial cation binding step during transport.

To determine whether individual TMHs of rOCT1 move in response to changes of the membrane potential, during cation binding and/or cation translocation we performed voltage-clamp fluorometry with transporter variants that were fluorescence-labeled at amino acids of individual TMHs that are located at the boundary between plasma membrane and extracellular aqueous phase [50, 60]. The experiments were performed with a rOCT1 variant in which all cysteine residues with exception of those forming the disulfide bridges in the large extracellular loop had been removed [48]. In this variant individual amino acids were replaced by cysteine and the introduced cysteine residue was labeled with the covalently binding fluorescent dye tetramethylrhodamine-6-maleimide. We observed membrane potential-dependent movements of TMHs 5, 8 and 11 which were partially or totally reversed by addition of transported cations or of the non-transported cationic inhibitor

TBuA. Potential-dependent movements of TMH 11 were strongly effected by choline, MPP and only slightly influencd by TBuA. At variance choline, MPP and TBuA induced differential effects on potential-dependent movements of TMH 8. The data indicate potential-dependent structural changes of rOCT1 that involve TMHs 5, 8 and 11. The open, outward-facing conformation of rOCT1 is supposed be the predominant conformation at the physiological membrane potential around −50 mV because it allowed rapid and complete inhibition of rOCT1 by extracellular TBuA. This conformation—or equilibrium of conformations—is changed after binding of TBuA and probably also after binding of choline and MPP. The similar movements of TMH 11 observed with choline, MPP and TBuA suggest that TMH 11 is involved in transport related conformational changes independently of the structure of the interacting cation. The cation specific movements of TMH 5 and 8 indicate cation specific structural movements.

Identification of a Substrate Binding Hinge Domain in OCTs

Our data suggested an important role of TMH 11 during cation translocation. First, movements of TMH 11 were induced by the three tested compounds choline, MPP and TBuA [60]. Second, exchange of Asp475 in the middle of TMH 11 by glutamate decreased V_{max} for TEA and MPP and changed substrate selectivity [44]. Third, also the exchange of Phe483 at the transition of TMH 11 to the extracellular space changed cation selectivity [60]. Fourth, exchange of Cys474 in hOCT2 by alanine increased the affinity for TEA [61], and fifth, the Gly447–Gly448 motif in TMH11 suggests mobility for bending of the α-helix that may be required for the transition between open and closed states of the transporter [60].

When the freedom for bending of TMH 11 was reduced by exchange of Gly448 with cysteine, uptake of MPP was decreased whereas the K_m for MPP was not changed [60]. In addition, the voltage dependent movement of TMH was blocked [60]. The data suggest that a decrease of flexibility in the middle of TMH 11 impairs movement of TMH 11 and transport activity of structurally different cations. The open outward-facing model of rOCT1 suggests that Asp475 and Phe160 form part of the entrance to the innermost cavity of the outward-facing cleft (Fig. 2.3a, b). Trying to verify this aspect of the structural model, we investigated whether access of cations can be blocked by covalent labeling of a cysteine residue that was introduced in position 448, with the covalent binding substrate analog tetramethylrhodamine-6-maleimide. The location of Gly448 within or close to a transport-relevant cation binding center was indicated by the observation that the covalent labeling of rOCT1(G478C) mutant was partially blocked by transported cations. After covalent labeling of Cys478 with tetramethylrhodamine-6-maleimide cation transport was largely reduced. This can be explained by blockage of cation access to the innermost cavity of the outward-facing cleft or by blockage of transporter related conformational changes. Taken together the data indicate that the motif CDXGGI that is conserved in OCT1-3 but not in OCTNs or OATs represents an OCT specific substrate binding hinge domain.

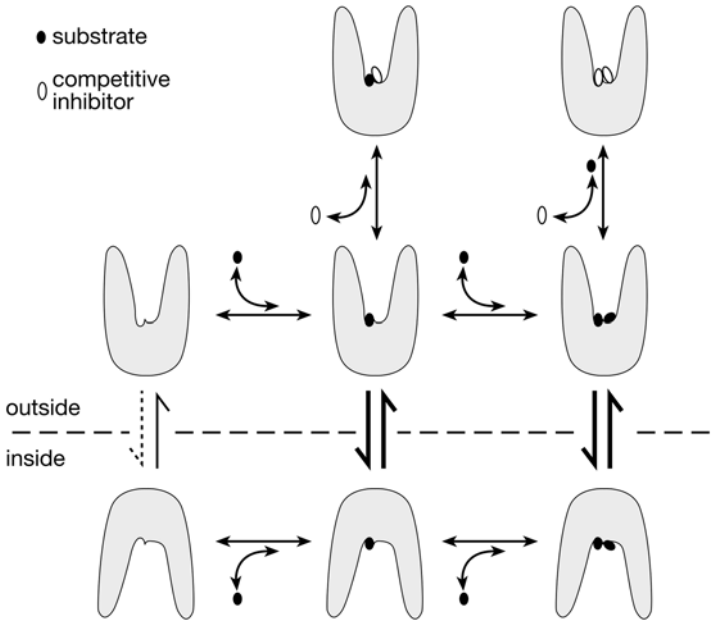

Fig. 2.3 Proposed mechanism for translocation of small organic cations by rOCT1 in the one cation/monomer and two cations/monomer modes, and for inhibition of transport by a competitive inhibitor. The two low-affinity transport-relevant cation binding sites are indicated whereas the high-affinity binding site is not shown. Both low-affinity sites are closely associated. After loading of the outward-facing cleft with one or two cationic substrates the equilibrium of rOCT1 conformations may change in favour of an inward open conformation. In the inward open conformation one or both cationic substrates may be released. The inward open transporter conformation may change to the outward open state in loaded forms or in the unloaded state. A competitive inhibitor applied from extracellular may inhibit cation uptake with different affinities if the transporter operates in one cation/monomer mode or two cations/monomer mode. The affinity for inhibition of the one cation/monomer mode may be also dependent on the structure of the employed substrate

Effect of Mutations on the Binding of MPP to rOCT1 Reconstituted into Nanodiscs

Recently we succeeded to measure binding of radioactively labeled MPP to purified rOCT1 which was reconstituted into nanodiscs consisting of a lipid bilayer that is framed by the amphiphilic membrane scaffold protein MSP1 (T. Keller, F. Bernhard, V. Doetsch, V. Gorboulev, H. Koepsell, unpublished data) [62]. Cell-free expressed rOCT1 was co-translationally incorporated into the nanondiscs [56, 62, 63], and binding of different concentrations of MPP was measured using a filter assay. The lipid bilayer consisted of di-myristoyl phosphatidylcholine (DMPG) or palmitoyl-oleyl phoshatidylcholine (POPC). The amount of rOCT1 protein in the nanodiscs was measured by quantification of Western blots, and dissociation constants (K_D) and maximal binding (B_{max}) were determined. In parallel, cell-free expressed rOCT1

was reconstituted into proteoliposomes formed from phosphatidylcholine, phosphatidylserine and cholesterol [56], and the apparent K_m and V_{max} values were calculated.

After reconstitution of rOCT1 wildtype into nanodiscs formed from DMPG or after reconstitution of a rOCT1 variant in which oligomerization was prevented by replacement of the cysteine residues in the large extracellular loop (rOCT1-6ΔC) [57], binding of two MPP molecules per rOCT1 monomer and one K_D of about 30 μM was determined (T. Keller, F. Bernhard, V. Doetsch, V. Gorboulev, H. Koepsell, unpublished data). However, when rOCT1 or rOCT1-6ΔC was reconstituted in nanodiscs that were formed with POPC, binding of three molecules MPP per rOCT1 monomer was observed. For binding of two MPP molecules a common low affinity K_D of 36 μM was obtained whereas for binding of the third MPP molecule a high affinity K_D of 0.24 μM were determined. For MPP transport into proteoliposomes reconstituted with rOCT1 wildtype only one K_m of 19 μM was resolved. The data suggest that the interaction of MPP with two low affinity MPP binding sites per rOCT1 monomer is relevant for transport.

We also measured MPP binding to rOCT1 mutants that were reconstituted into nanodiscs formed with POPC as well as MPP uptake by rOCT1 mutants that were reconstituted into proteoliposomes. First we exchanged Asp475 or Tryp218 which are located in the same region of the modeled outward-facing cleft of rOCT1 (Fig. 2.2a, b). We observed that only two MPP molecules bound per OCT1 monomer when either Trp218 was replaced by tyrosine (rOCT1-W218Y) or when Asp475 was replaced by glutamate (rOCT1-D475E). Whereas in both mutants the K_D value of the high affinity site remained unchanged, the K_D value of the low affinity site was decreased by 50 % in rOCT1-W218Y and by 25 % in rOCT1-D475E. The K_m values determined for mutants rOCT1-W218F and rOCT1-D475E were similar to rOCT1 wildtype, however, the turnover numbers were decreased by 50 % in rOCT1-W218F and by 80 % in rOCT1-D475E.

We also investigated the effects of replacements of Leu447 by phenylalanine or tyrosine (T. Keller, F. Bernhard, V. Doetsch, V. Gorboulev, H. Koepsell, unpublished data). Leu447 is located in a different region of the outward-facing binding cleft of rOCT1 than Asp475 and Trp218 (Fig. 2.2a, b). The mutations of Leu447 did not change total binding of three MPP molecules per transporter monomer observed in rOCT1 wildtype. Also the K_D value for high affinity MPP binding was not significantly different compared to rOCT1 wildtype. At variance, the K_D of the low affinity site was 2.5-fold decreased in rOCT1-L447F and 4.6-fold decreased in rOCT1-L477Y. For MPP transport by rOCT1-L447F and rOCT1-L447Y twofold lower K_m values compared to rOCT1 wildtype were observed whereas turnover numbers were similar.

The data indicate that the structure of the substrate binding region of rOCT1 is dependent on the lipid environment of rOCT1. Because the K_m value for rOCT1 mediated MPP transport measured in proteoliposomes is about fourfold higher compared to the K_m value of rOCT1 mediated MPP transport measured in cells, and the K_D value for low-affinity MPP binding to rOCT1 determined in nanodiscs is 40-fold higher compared to high-affinity MPP binding to a cysteine-less rOCT1

determined by voltage-clamp fluorometry (see below), the structure of the cation binding region may be modulated by various factors in cells that have not been mimicked after reconstitution in nanodiscs and/or proteoliposomes. In addition to a different lipid microenvironment in cellular membranes the structure of the binding region may be influenced by phosphorylation of rOCT1 in cells [64] and by interaction with cellular proteins [65]. Also the replacements of endogenous cysteine residues in rOCT1, the exchange of Phe483 by cysteine, and fluorescence labeling of cysteine in position 483 performed in the rOCT1 variant used for voltage-clamp fluorometry (see below), may have had an effect on the binding regions. However, in spite of the differences in absolute binding affinities observed with the different methods, the cell-free expressed transporter reconstituted in lipid bilayers of appropriate phospholipids provides an excellent model to study structure-function relationship of binding and transport.

After reconstitution into nanodiscs rOCT1 can bind MPP in the outward-facing and inward-facing conformation. After binding to the outward-facing conformation or after binding to the inward conformation MPP may be transported to the other side of the nanodiscs, however, since MPP in the aqueous phase is removed during the filter binding-assay, only MPP molecules are detected that are bound to the transporter. Because the outward- and inward-facing conformations are mutually exclusive, the determined stoichiometry indicates that three MPP molecules bind per binding cleft of rOCT1 monomer. We interprete that the high-affinity and low-affinity binding sites for MPP characterized in nanodiscs are located in the outward-facing binding cleft. One reason is that rOCT1 is mainly involved in cellular cation uptake, and that the cation binding sites for MPP in cellular uptake systems are supposed to have a higher affinity in the outward-facing compared to the inward-facing conformation. Other reasons are that we detected high-affinity and low-affinity cation binding sites in rOCT1 after application of the non-transported cationic inhibitor TBuA from extracellular [50] and that we observed high-affinity and low-affinity binding sites for inhibition of cation uptake by human OCTs after application of transported cationic drugs from extracellular [66].

From the observed effects of mutations of amino acids located in the innermost part of the outward-facing binding cleft important conclusions can be drawn. The data indicate that Tryp218 and Asp475 are directly or indirectly involved in MPP binding to one transport relevant low-affinity MPP binding site. After mutations in both positions the number of MPP molecules bound per monomer was decreased from three to two, and the K_D for low-affinity MPP binding was changed. In addition both mutants showed a decreased turnover number for MPP transport. Leu447 appears to be located close to the second transport relevant low-affinity MPP binding site. Mutations in this position decreased the affinity of low-affinity MPP binding and the K_m of MPP transport. Because mutations in this position did not reduce the number of MPP molecules bound per rOCT1 monomer Leu447 is probably not directly involved in MPP binding to the second low-affinity MPP binding site. The observation that the K_D of high-affinity MPP binding was not altered after the performed mutation suggests that the high-affinity site is not located within the innermost part of the outward-facing cleft. Our data do not allow to distinguish whether the high-affinity site is regulatory or directly involved in transport.

Identification of High-Affinity Cation Binding Sites of rOCT1 by Voltage-Clamp Fluorometry

We employed cation induced voltage-dependent fluorescence changes of a fluorescent labeled rOCT1 variant to determine affinities for the binding of the substrates choline, TEA, MPP, and the non-transported inhibitor TBuA [50]. In the rOCT1 variant all cysteine residues with exception of the six cysteine residues in the large extracellular loop were removed and one reactive cysteine residue was introduced in position 483 that was covalently labeled with the fluorescent sulfhydryl reagent tetramethylrhodamine-6-maleimide. For choline, TEA and MPP two individual binding sites with low and high affinities were titrated [50]. The apparent K_D values of the low affinity sites (choline 0.35 mM, TEA 57 μM, MPP 0.87 μM) were in the range of the apparent K_m values determined for transport of the respective cations or the K_i values determined for inhibition of transport measured in cells in which rOCT1 was overexpressed. For the high affinity sites, K_D values of 12 nM (choline), 57 nM (TEA) and 41 pM (MPP) were determined by voltage-clamp fluorometry. Notably the high afffinity K_D value for MPP is 6000-fold lower compared to the high affinity K_D value determined for rOCT1 wildtype in nanodiscs. For the non-transported inhibitor TBuA three different binding sites were distinguished. One apparent K_D value (0.3 μM) is ten times lower than the apparent K_i value for inhibition of TEA uptake measured in oocytes [44] and three times lower than the apparent K_i value for inhibition of MPP uptake measured in HEK293 cells (H. Koepsell and V. Gorboulev, unpublished data). The other apparent K_D values determined by voltage-clamp fluorometry (~0.4 nM and ~2 pM) indicate binding sites with very high affinities.

Hypothesis on Mechanism of Substrate Binding and Translocation by rOCT1

The above described data indicate that each rOCT1 monomer is capable to bind three molecules of MPP. The changes in binding and transport observed in rOCT1 mutants suggest that two low-affinity MPP binding sites located in close proximity within the innermost part of the outward-facing cleft are involved in transport. This interpretation is based on the following observations. First, mutations of Trp218 and Asp475 that are located in one region within the innermost part of the modeled outward-facing cleft (Fig. 2.2a, b), destroy one low affinity MPP binding site, change the K_D for MPP binding to the remaining low-affinity site, and halve the turnover for MPP uptake. Second, mutations of Leu447 which is located in a different niche of the inner part of the modeled outward-facing cleft (Fig. 2.2a, b), do not destroy a low-affinity binding site but also change the K_D for low-affinity binding which is supposed to represent a lumped constant for binding to both low-affinity MPP binding sites. Our data suggest that rOCT1 mediated translocation of MPP

may occur when one or both low-affinity MPP binding sites of the monomer are loaded i.e. in a one cation/monomer transport mode and in the two cation/monomer transport mode. This hypothesis is depicted in Fig. 2.3. The capability of rOCT1 to operate in a one cation/monomer mode is supported by the observation that transport was observed when one low-affinity MPP binding site was blocked after mutation of D475 or W218. The capability of rOCT1 to operate in a two cation/monomer transport mode is suggested by the observation that the optimal turnover of rOCT1 was only observed when both low-affinity binding sites were intact. Operation in the one cation/monomer mode at substrate concentrations far below the lumped K_D value of both low-affinity binding sites and operation in the two cation/monomer mode at saturating substrate concentration is suggested by the observation that the substrate dependence of MPP uptake by rOCT1 wildtype and by the L447 mutants was hyperbolic rather than exponential as would be expected if the transporter would only function in the two cation/monomer mode.

Considering the complex structure of the transport relevant cation binding region one can imagine that also two different organic cations may be transported together. It appears to be also possible that larger substrates are only transported in the one/monomer transport mode. The proposed one/monomer and two/monomer transport mode for small cations increases the versatile capability of rOCT1 to mediate uptake at largely differing concentrations of extracellular substrates.

Potential Mechanisms for Inhibition of rOCT1 Mediated Transport

Based on the complex mechanism of organic cation transport by OCTs involving one cation/monomer and two cation/monomer transport modes and the existence of high affinity cation binding sites that may be regulatory, various ways can be imagined how transport can be slowed down or blocked by transported or nontransported inhibitors. Because all transported cations have to bind at transport relevant binding sites within the innermost part of the outward-facing binding cleft, which represent low-affinity binding sites in case of MPP and rOCT1, mutual competition at these sites should be an important mechanism for inhibition. At substrate concentrations above K_m, when small substrates may be translocated predominantly in the two cation/monomer mode and the high-affinity substrate binding site(s) should be loaded, the K_i values of transported inhibitors and competitive nontransported inhibitors should be relatively independent from the substrate employed for uptake measurements because inhibition is supposed to be mainly due to substrate replacement at the transport sites (Fig. 2.3). At variance, when very small substrate concentrations are used for inhibition studies i.e. when mainly inhibition of the one cation/monomer transport mode is measured, inhibitors may not only compete with the substrate loaded low-affinity binding site but may also interact with the second unoccupied low-affinity binding site and inhibit transport without replacement of

the substrate (Fig. 2.3). If the substrate bound to one low-affinity site contains hydrophobic aromatic rings such as MPP, the interaction of hydrophobic competitive inhibitors may include interaction with the bound substrate (Fig. 2.3). Due to the proximity of both cation binding sites allowing short range effects of substrate binding to one low-affinity site on the structure of the second low-affinity site and/or interaction of the inhibitor with the bound hydrophobic cation, the affinity of inhibitor binding to the transporter monomer containing one substrate may be higher compared to the unloaded monomer. At very low substrate concentrations transport inhibition via interaction of inhibitors with high affinity cation binding sites may be possible via allosteric effects on transport.

In the frame of the proposed model for transport in two modes recent experimental data of biomedical impact that appeared to be incomprehensible on the first view can be explained. Measuring inhibition of MPP uptake mediated by human OCT1, OCT2 and OCT3 with the antiviral drug lamuvidine, monophasic inhibition curves were obtained when MPP concentrations near the K_m of MPP were used for uptake measurements, whereas biphasic inhibition curves indicating high-affinity and low-affinity inhibitor binding sites were resolved when the MPP concentration employed for the uptake measurements was far below the K_m of MPP [66]. Lamuvidine which is transported by human OCT1-3 with apparent K_m values between 1.3 and 2.1 mM inhibited the uptake of 1.3 nM MPP by human OCT1-3 about 50 % with a half maximal effective concentrations (EC_{50}) values between 8 and 20 pM and inhibited the remaining 50 % with EC_{50} values between 1.9 and 3.5 mM [66]. The transport model depicted in Fig. 2.3 also provides an intuitive plausible explanation for the recently reported observation that largely different affinities of OCT inhibitors were determined when very low concentrations of different substrates were used for the uptake measurements [67–69]. This property of OCTs is of high biomedical importance for the prediction of clinical drug–drug interactions. In the one cation/monomer transport mode prevailing at very low substrate concentration, the inhibitors may interact with a transport relevant low-affinity binding site that has been differentially modified due to binding of different substrates to the second transport relevant binding site, and/or the affinity may be increased by hydrophobic interaction with bound substrate.

Concluding Remarks

The outlined concept concerning polyspecific substrate binding to OCTs, translocation of substrates and inhibition of transport has been derived from recent reported crystal structures of transporters of the MFS, detailed functional characterization of rOCT1 and rOCT2, extensive mutagenesis, and recent MPP binding measurements that allowed the identification of three MPP binding sites per rOCT1 monomer. This transport model provides intuitively convincing explanations for the observations that largely different inhibitor sensitivities were determined for transport at very low substrate concentrations compared to transport at substrate concentrations around

the K_m values and that inhibitor sensitivities measured at very low substrate concentrations were largely different when different substrates were used for the uptake measurements. Providing a comprehensible model for these observations will help pharmacists to accept these new alarming properties that have to be considered for preclinical in vitro testing of drug–drug interactions. The molecular understanding how the polyspecific organic cation transporters of the SLC22 family operate in general and which specific features can be attributed to the three human OCTs is of high theoretical interest and has high biomedical impact. The presented model provides a frame for future mutagenesis experiments. The observed functional effects of the mutations will help to develop a more defined and less hypothetical model when crystals structures of different functional states of transporters of the SLC22 family, the SLC22 subfamily of OCTs and of individual OCT subtypes will be available. Considering the fact that so far no crystal structure of a mammalian transporter of the MFS has been reported it will be still a long way to go. However, this is the only possibility to develop a solid basis for in silico drug design and to establish more predictive high throughput procedures for drug testing.

References

1. Gründemann D, Gorboulev V, Gambaryan S, Veyhl M, Koepsell H. Drug excretion mediated by a new prototype of polyspecific transporter. Nature. 1994;372:549–52.
2. Koepsell H, Lips K, Volk C. Polyspecific organic cation transporters: structure, function, physiological roles, and biopharmaceutical implications. Pharm Res. 2007;24:1227–51.
3. Koepsell H. The SLC22 family with transporters of organic cations, anions and zwitterions. Mol Aspects Med. 2013;34:413–35.
4. Pao SS, Paulsen IT, Saier Jr MH. Major facilitator superfamily. Microbiol Mol Biol Rev. 1998;62:1–34.
5. Schmitt BM, Gorbunov D, Schlachtbauer P, Egenberger B, Gorboulev V, Wischmeyer E, Müller T, Koepsell H. Charge-to-substrate ratio during organic cation uptake by rat OCT2 is voltage dependent and altered by exchange of glutamate 448 with glutamine. Am J Physiol Renal Physiol. 2009;296:F709–22.
6. Koepsell H, Schmitt BM, Gorboulev V. Organic cation transporters. Rev Physiol Biochem Pharmacol. 2003;150:36–90.
7. Arndt P, Volk C, Gorboulev V, Budiman T, Popp C, Ulzheimer-Teuber I, Akhoundova A, Koppatz S, Bamberg E, Nagel G, Koepsell H. Interaction of cations, anions, and weak base quinine with rat renal cation transporter rOCT2 compared with rOCT1. Am J Physiol Renal Physiol. 2001;281:F454–68.
8. Chen R, Jonker JW, Nelson JA. Renal organic cation and nucleoside transport. Biochem Pharmacol. 2002;64:185–90.
9. Busch AE, Quester S, Ulzheimer JC, Gorboulev V, Akhoundova A, Waldegger S, Lang F, Koepsell H. Monoamine neurotransmitter transport mediated by the polyspecific cation _transporter rOCT1. FEBS Lett. 1996;395:153–6.
10. Busch AE, Quester S, Ulzheimer JC, Waldegger S, Gorboulev V, Arndt P, Lang F, Koepsell H. Electrogenic properties and substrate specificity of the polyspecific rat cation transporter rOCT1. J Biol Chem. 1996;271:32599–604.
11. Nagel G, Volk C, Friedrich T, Ulzheimer JC, Bamberg E, Koepsell H. A reevaluation of substrate specificity of the rat cation transporter rOCT1. J Biol Chem. 1997;272:31953–6.

12. Budiman T, Bamberg E, Koepsell H, Nagel G. Mechanism of electrogenic cation transport by the cloned organic cation transporter 2 from rat. J Biol Chem. 2000;275:29413–20.
13. Keller T, Elfeber M, Gorboulev V, Reiländer H, Koepsell H. Purification and functional reconstitution of the rat organic cation transporter OCT1. Biochemistry. 2005;44:12253–63.
14. Schmitt BM, Koepsell H. Alkali cation binding and permeation in the rat organic cation transporter rOCT2. J Biol Chem. 2005;280:24481–90.
15. Diez-Sampedro A, Hirayama BA, Osswald C, Gorboulev V, Baumgarten K, Volk C, Wright EM, Koepsell H. A glucose sensor hiding in a family of transporters. Proc Natl Acad Sci U S A. 2003;100:11753–8.
16. Accardi A, Miller C. Secondary active transport mediated by a prokaryotic homologue of ClC Cl^- channels. Nature. 2004;427:803–7.
17. Dutzler R, Campbell EB, Cadene M, Chait BT, MacKinnon R. X-ray structure of a ClC chloride channel at 3.0 A reveals the molecular basis of anion selectivity. Nature. 2002;415:287–94.
18. Miller C. ClC chloride channels viewed through a transporter lens. Nature. 2006;440:484–9.
19. Jardetzky O. Simple allosteric model for membrane pumps. Nature. 1966;211:969–70.
20. Law CJ, Maloney PC, Wang D-N. Ins and outs of major facilitator superfamily antiporters. Annu Rev Microbiol. 2008;62:289–305.
21. Volk C, Gorboulev V, Budiman T, Nagel G, Koepsell H. Different affinities of inhibitors to the outwardly and inwardly directed substrate binding site of organic cation transporter 2. Mol Pharmacol. 2003;64:1037–47.
22. Dang S, Sun L, Huang Y, Lu F, Liu Y, Gong H, Wang J, Yan N. Structure of a fucose transporter in an outward-open conformation. Nature. 2010;467:734–8.
23. Sun L, Zeng X, Yan C, Sun X, Gong X, Rao Y, Yan N. Crystal structure of a bacterial homologue of glucose transporters GLUT1-4. Nature. 2012;490:361–6.
24. Hirai T, Heymann JAW, Shi D, Sarker R, Maloney PC, Subramaniam S. Three-dimensional structure of a bacterial oxalate transporter. Nat Struct Biol. 2002;9:597–600.
25. Yin Y, Jensen MØ, Tajkhorshid E, Schulten K. Sugar binding and protein conformational changes in lactose permease. Biophys J. 2006;91:3972–85.
26. Yan H, Huang W, Yan C, Gong X, Jiang S, Zhao Y, Wang J, Shi Y. Structure and mechanism of a nitrate transporter. Cell Rep. 2013;3:716–23.
27. Pedersen BP, Kumar H, Waight AB, Risenmay AJ, Roe-Zurz Z, Chau BH, Schlessinger A, Bonomi M, Harries W, Sali A, Johri AK, Stroud RM. Crystal structure of a eukaryotic phosphate transporter. Nature. 2013;496:533–6.
28. Newstead S, Drew D, Cameron AD, Postis VL, Xia X, Fowler PW, Ingram JC, Carpenter EP, Sansom MS, McPherson MJ, Baldwin SA, Iwata S. Crystal structure of a prokaryotic homologue of the mammalian oligopeptide-proton symporters, PepT1 and PepT2. EMBO J. 2011;30:417–26.
29. Abramson J, Smirnova I, Kasho V, Verner G, Kaback HR, Iwata S. Structure and mechanism of the lactose permease of *Escherichia coli*. Science. 2003;301:610–5.
30. Mirza O, Guan L, Verner G, Iwata S, Kaback HR. Structural evidence for induced fit and a mechanism for sugar/H^+ symport in LacY. EMBO J. 2006;25:1177–83.
31. Guan L, Mirza O, Verner G, Iwata S, Kaback HR. Structural determination of wild-type lactose permease. Proc Natl Acad Sci U S A. 2007;104:15294–8.
32. Chaptal V, Kwon S, Sawaya MR, Guan L, Kaback HR, Abramson J. Crystal structure of lactose permease in complex with an affinity inactivator yields unique insight into sugar recognition. Proc Natl Acad Sci U S A. 2011;108:9361–6.
33. Huang Y, Lemieux MJ, Song J, Auer M, Wang D-N. Structure and mechanism of the glycerol-3-phosphate transporter from *Escherichia coli*. Science. 2003;301:616–20.
34. Solcan N, Kwok J, Fowler PW, Cameron AD, Drew D, Iwata S, Newstead S. Alternating access mechanism in the POT family of oligopeptide transporters. EMBO J. 2012;31:3411–21.

35. Guettou F, Quistgaard EM, Tresaugues L, Moberg P, Jegerschold C, Zhu L, Jong AJ, Nordlund P, Low C. Structural insights into substrate recognition in proton-dependent oligopeptide transporters. EMBO Rep. 2013;14:804–10.
36. Doki S, Kato HE, Solcan N, Iwaki M, Koyama M, Hattori M, Iwase N, Tsukazaki T, Sugita Y, Kandori H, Newstead S, Ishitani R, Nureki O. Structural basis for dynamic mechanism of proton-coupled symport by the peptide transporter POT. Proc Natl Acad Sci U S A. 2013;110:11343–8.
37. Zheng H, Wisedchaisri G, Gonen T. Crystal structure of a nitrate/nitrite exchanger. Nature. 2013;497:647–51.
38. Sun J, Bankston JR, Payandeh J, Hinds TR, Zagotta WN, Zheng N. Crystal structure of the plant dual-affinity nitrate transporter NRT1.1. Nature. 2014;507:73–7.
39. Radestock S, Forrest LR. The alternating-access mechanism of MFS transporters arises from inverted-topology repeats. J Mol Biol. 2011;407:698–715.
40. Martin C, Berridge G, Higgins CF, Mistry P, Charlton P, Callaghan R. Communication between multiple drug binding sites on P-glycoprotein. Mol Pharmacol. 2000;58:624–32.
41. Aller SG, Yu J, Ward A, Weng Y, Chittaboina S, Zhuo R, Harrell PM, Trinh YT, Zhang Q, Urbatsch IL, Chang G. Structure of P-glycoprotein reveals a molecular basis for poly-specific drug binding. Science. 2009;323:1718–22.
42. Klingenberg M. Ligand-protein interaction in biomembrane carriers. The induced transition fit of transport catalysis. Biochemistry. 2005;44:8563–70.
43. Klingenberg M. Transport catalysis. Biochim Biophys Acta. 2006;1757:1229–36.
44. Gorboulev V, Volk C, Arndt P, Akhoundova A, Koepsell H. Selectivity of the polyspecific cation transporter rOCT1 is changed by mutation of aspartate 475 to glutamate. Mol Pharmacol. 1999;56:1254–61.
45. Popp C, Gorboulev V, Müller TD, Gorbunov D, Shatskaya N, Koepsell H. Amino acids critical for substrate affinity of rat organic cation transporter 1 line the substrate binding region in a model derived from the tertiary structure of lactose permease. Mol Pharmacol. 2005;67:1600–11.
46. Gorboulev V, Shatskaya N, Volk C, Koepsell H. Subtype-specific affinity for corticosterone of rat organic cation transporters rOCT1 and rOCT2 depends on three amino acids within the substrate binding region. Mol Pharmacol. 2005;67:1612–9.
47. Volk C, Gorboulev V, Kotzsch A, Müller TD, Koepsell H. Five amino acids in the innermost cavity of the substrate binding cleft of organic cation transporter 1 interact with extracellular and intracellular corticosterone. Mol Pharmacol. 2009;76:275–89.
48. Sturm A, Gorboulev V, Gorbunov D, Keller T, Volk C, Schmitt BM, Schlachtbauer P, Ciarimboli G, Koepsell H. Identification of cysteines in rat organic cation transporters rOCT1 (C322, C451) and rOCT2 (C451) critical for transport activity and substrate affinity. Am J Physiol Renal Physiol. 2007;293:F767–79.
49. Abramson J, Smirnova I, Kasho V, Verner G, Iwata S, Kaback HR. The lactose permease of *Escherichia coli*: overall structure, the sugar-binding site and the alternating access model for transport. FEBS Lett. 2003;555:96–101.
50. Gorbunov D, Gorboulev V, Shatskaya N, Mueller T, Bamberg E, Friedrich T, Koepsell H. High-affinity cation binding to organic cation transporter 1 induces movement of helix 11 and blocks transport after mutations in a modeled interaction domain between two helices. Mol Pharmacol. 2008;73:50–61.
51. Ambudkar SV, Anantharam V, Maloney PC. UhpT, the sugar phosphate antiporter of *Escherichia coli*, functions as a monomer. J Biol Chem. 1990;265:12287–92.
52. Sahin-Toth M, Lawrence MC, Kaback HR. Properties of permease dimer, a fusion protein containing two lactose permease molecules from *Escherichia coli*. Proc Natl Acad Sci U S A. 1994;91:5421–5.
53. Hou Z, Cherian C, Drews J, Wu J, Matherly LH. Identification of the minimal functional unit of the homo-oligomeric human reduced folate carrier. J Biol Chem. 2010;285:4732–40.

54. Veenhoff LM, Heuberger EH, Poolman B. The lactose transport protein is a cooperative dimer with two sugar translocation pathways. EMBO J. 2001;20:3056–62.
55. Hong M, Xu W, Yoshida T, Tanaka K, Wolff DJ, Zhou F, Inouye M, You G. Human organic anion transporter hOAT1 forms homooligomers. J Biol Chem. 2005;280:32285–90.
56. Keller T, Schwarz D, Bernhard F, Dotsch V, Hunte C, Gorboulev V, Koepsell H. Cell free expression and functional reconstitution of eukaryotic drug transporters. Biochemistry. 2008;47:4552–64.
57. Keller T, Egenberger B, Gorboulev V, Bernhard F, Uzelac Z, Gorbunov D, Wirth C, Koppatz S, Dötsch V, Hunte C, Sitte HH, Koepsell H. The large extracellular loop of organic cation transporter 1 influences substrate affinity and is pivotal for oligomerization. J Biol Chem. 2011;286:37874–86.
58. Brast S, Grabner A, Sucic S, Sitte HH, Hermann E, Pavenstadt H, Schlatter E, Ciarimboli G. The cysteines of the extracellular loop are crucial for trafficking of human organic cation transporter 2 to the plasma membrane and are involved in oligomerization. FASEB J. 2012;26:976–86.
59. Duan P, Li S, You G. Transmembrane peptide as potent inhibitor of oligomerization and function of human organic anion transporter 1. Mol Pharmacol. 2011;79:569–74.
60. Egenberger B, Gorboulev V, Keller T, Gorbunov D, Gottlieb N, Geiger D, Mueller TD, Koepsell H. A substrate binding hinge domain is critical for transport-related structural changes of organic cation transporter 1. J Biol Chem. 2012;287:31561–73.
61. Pelis RM, Dangprapai Y, Cheng Y, Zhang X, Terpstra J, Wright SH. Functional significance of conserved cysteines in the human organic cation transporter 2. Am J Physiol Renal Physiol. 2012;303:F313–20.
62. Raschle T, Hiller S, Yu TY, Rice AJ, Walz T, Wagner G. Structural and functional characterization of the integral membrane protein VDAC-1 in lipid bilayer nanodiscs. J Am Chem Soc. 2009;131:17777–9.
63. Roos C, Zocher M, Muller D, Munch D, Schneider T, Sahl HG, Scholz F, Wachtveit J, Ma Y, Proverbio D, Henrich E, Dotsch V, Bernhard F. Characterization of co-translationally formed nanodisc complexes with small multidrug transporters, proteorhodopsin and with the *E. coli* MraY translocase. Biochim Biophys Acta. 2012;1818:3098–106.
64. Ciarimboli G, Koepsell H, Iordanova M, Gorboulev V, Dürner B, Lang D, Edemir B, Schröter R, Van Le T, Schlatter E. Individual PKC-phosphorylation sites in organic cation transporter 1 determine substrate selectivity and transport regulation. J Am Soc Nephrol. 2015;16:1562–70.
65. Grabner A, Brast S, Sucic S, Bierer S, Hirsch B, Pavenstädt H, Sitte HH, Schlatter E, Ciarimboli G. *LAPTM4A* interacts with *hOCT2* and regulates its endocytotic recruitment. Cell Mol Life Sci. 2011;68:4079–90.
66. Minuesa G, Volk C, Molina-Arcas M, Gorboulev V, Erkizia I, Arndt P, Clotet B, Pastor-Anglada M, Koepsell H, Martinez-Picado J. Transport of lamivudine [(-)-b-L-2′,3′-dideoxy-3′-thiacytidine] and high-affinity interaction of nucleoside reverse transcriptase inhibitors with human organic cation transporters 1, 2, and 3. J Pharmacol Exp Ther. 2009;329:252–61.
67. Nies AT, Koepsell H, Damme K, Schwab M. Organic cation transporters (OCTs, MATEs), in vitro and in vivo evidence for the importance in drug therapy. Handb Exp Pharmacol. 2010;201:105–67.
68. Thevenod F, Ciarimboli G, Leistner M, Wolff NA, Lee WK, Schatz I, Keller T, Al-Monajjed R, Gorboulev V, Koepsell H. Substrate- and cell contact-dependent inhibitor affinity of human organic cation transporter 2: studies with two classical organic cation substrates and the novel substrate Cd. Mol Pharm. 2013;10:3045–56.
69. Belzer M, Morales M, Jagadish B, Mash EA, Wright SH. Substrate-dependent ligand inhibition of the human organic cation transporter OCT2. J Pharmacol Exp Ther. 2013;346:300–10.

http://www.springer.com/978-3-319-23792-3

Organic Cation Transporters
Integration of Physiology, Pathology, and Pharmacology
Ciarimboli, G.; Gautron, S.; Schlatter, E. (Eds.)
2016, XV, 264 p. 34 illus., 14 illus. in color., Hardcover
ISBN: 978-3-319-23792-3